

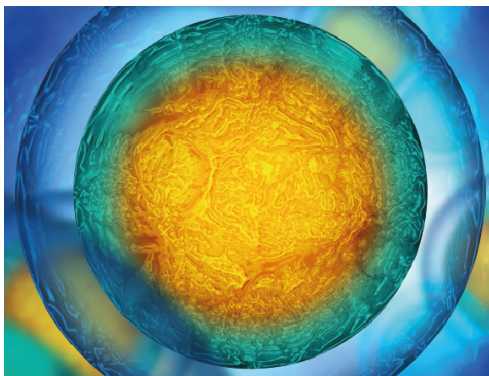


PAPER • OPEN ACCESS

Chondrobags: A high throughput alginate-fibronectin micromass platform for *in vitro* human cartilage formation

To cite this article: Kimia Witte *et al* 2020 *Biofabrication* **12** 045034

View the [article online](#) for updates and enhancements.



Biophysical Society

IOP | ebooks™

Your publishing choice in all areas of biophysics research.

Start exploring the collection—download the first chapter of every title for free.



PAPER

OPEN ACCESS

RECEIVED
10 July 2020REVISED
26 August 2020ACCEPTED FOR PUBLICATION
8 September 2020PUBLISHED
30 September 2020

Original content from
this work may be used
under the terms of the
[Creative Commons
Attribution 4.0 licence](#).

Any further distribution
of this work must
maintain attribution to
the author(s) and the title
of the work, journal
citation and DOI.



Chondrobags: A high throughput alginate-fibronectin micromass platform for *in vitro* human cartilage formation

Kimia Witte^{1,2} , María C de Andrés^{3,4} , Julia Wells³ , Matthew J Dalby¹ , Manuel Salmeron-Sanchez¹
and Richard O C Oreffo^{3,5}

¹ Centre for the Cellular Microenvironment, University of Glasgow, Glasgow, United Kingdom

² Strathclyde Institute of Pharmacy and Biomedical Sciences, University of Strathclyde, Glasgow, United Kingdom

³ Centre for Human Development, Stem Cells and Regeneration, Institute of Developmental Sciences, Faculty of Medicine, University of Southampton, Southampton, United Kingdom

⁴ INIBIC-Complejo Hospitalario Universitario A Coruña (CHUAC), Rheumatology Division, A Coruña, Spain

⁵ College of Biomedical Engineering, China Medical University, Taichung 40402, Taiwan

E-mail: Richard.Oreffo@soton.ac.uk

Keywords: biofabrication, droplet-based microfluidics, stem cells, chondrogenesis, hydrogels, fibronectin

Supplementary material for this article is available [online](#)

Abstract

The maintenance and expansion of the cells required for formation of tissue-engineered cartilage has, to date, proven difficult. This is, in part, due to the initial solid phase extracellular matrix demanded by the cells inhabiting this avascular tissue. Herein, we engineer an innovative alginate-fibronectin microfluidic-based carrier construct (termed a chondrobag) equipped with solid phase presentation of growth factors that support skeletal stem cell chondrogenic differentiation while preserving human articular chondrocyte phenotype. Results demonstrate biocompatibility, cell viability, proliferation and tissue-specific differentiation for chondrogenic markers *SOX9*, *COL2A1* and *ACAN*. Modulation of chondrogenic cell hypertrophy, following culture within chondrobags loaded with TGF- β 1, was confirmed by down-regulation of hypertrophic genes *COL10A1* and *MMP13*. MicroRNAs involved in the chondrogenesis process, including miR-140, miR-146b and miR-138 were observed. Results demonstrate the generation of a novel high-throughput, microfluidic-based, scalable carrier that supports human chondrogenesis with significant implications therein for cartilage repair-based therapies.

1. Introduction

Cartilage lesions represent an important technical challenge for tissue engineering given the avascular nature of this tissue, which often leads to defective intrinsic healing [1]. Unattended cartilage damage can result in osteoarthritis (OA), the most prevalent chronic pathology of joints [1, 2]. Defective articular cartilage and alterations made to the state of bone at joint margins for instance, are among a diverse set of signs and symptoms associated with OA [3]. Chondrocytes, derived from the native tissue, have been examined as an apparent cell source of the formation of neocartilage.

Over the last decades, interest in stem cells for tissue engineering applications has noticeably increased,

given their capacity for self-renewal and multi-lineage differentiation [4]. Chondrocytes or chondroprogenitors, derived from stromal progenitors, need to be guided in the formation of native hyaline cartilage, to avert dedifferentiation and, critically, to ensure the generation of pre-eminent tissue reconstruction *in vivo* that resembles the complex cellular and extracellular matrix (ECM) make-up in the native tissue. In addition, the generated tissue must be permissive to typical load-bearing while providing long-lasting joint performance [5]. A wealth of literature suggests micromass or pellet culture models, offer an appropriate method for generating small-scale micron sized tissues of engineered neocartilage *in vitro*. Furthermore, more advanced cartilage-like tissues exhibiting improved mechanical properties have been

made exploiting 3D models for cell proliferation and differentiation [6]. These systems facilitate interactions between the cell and the requisite cellular environment/matrix [7]. However, these 3D systems still display an overall lack of homogeneity in cell responses related to the necrotic cores [8], that could be assigned to a list of contributing factors including: (i) the non-physiological closely compacted cells that are formed during initial stages of culture, (ii) the existence of necrotic cores enclosed by *in vitro/ex vivo* cell clusters as a consequence of high cell number, (iii) sub-standard physiological culture conditions and, (iv) diffusion limitations by uncontrolled establishment of chemical gradients throughout samples [9].

Recent studies have explored high throughput strategies for micro-tissue modeling [10, 11]. Thus, microfluidics offers significant potential for the generation of high-throughput cell culture prototypes, presenting unparalleled spatio-temporal control on the requisite micro-environmental conditions [12, 13]. To this objective, we present an experimental droplet-based microfluidic device for the fabrication and the culture of 3D micromass constructs of mature chondrocytes and skeletal stem cells (SSCs) generated under constant laminar flow, termed ‘chondrobags’. Chondrobags are highly mono-dispersed, pearl-lace interlinking hydrogel-based structures with pearl and lace subunit sizes ranging from 100 and 150 μm . We note that SSCs are a bone marrow derived multipotent mesenchymal stromal cell (MSCs) population with the established propensity for skeletal regeneration [14].

It is clear that materials used for cartilage tissue engineering significantly affect the pattern of the gene expression of the chondrocyte population therein [15]. Mimicking the hydrated environment of native cartilage, hydrogels offer an attractive approach for the development of cartilage regenerative strategies. Hydrogels are made by crosslinking naturally derived polymers, such as collagen and alginate, as well as polymers manufactured, such as polyethylene glycol and polyacrylamide. These polymer networks are crosslinked hydrophilic systems that are able to retain high volumes of fluid without dissolving. This allows construction of a microenvironment for cells, which takes on the appearance of native tissue through facilitation of waste and nutrients exchange [16]. Furthermore, hydrogels offer a strategy for the homogeneous encapsulation of cells of interest in comparison to numerous reported scaffolds. Critically, the mechanical properties of hydrogels, such as viscoelasticity, typically, can be fine-tuned to mimic those found in the native cartilage [17]. Alginate is a biocompatible material that is used to form microporous hydrogels [18]. The permeable nature of the alginate hydrogel allows diffusion of nutrients, molecules and facilitates communication and contact between cells, providing a rich ECM-like

environment that can support cell viability [19]. Indeed, a number of studies have shown that MSCs-laden alginate hydrogels can support chondrogenesis [19–21].

Naturally found alginate polymers offer good hydrophilicity and allow ionic crosslinking. However, alginate hydrogels lack intrinsic cell adhesion domains, which diminish their biological activity and subsequently hamper their use in tissue engineering [22]. Approaches to overcome this limitation have centred on the incorporation of molecules such as Arg-Gly-Asp (RGD)-based peptides to facilitate integrin binding [16]. The display of an RGD sequence in alginate hydrogels provides a strategy for control over the phenotype of participating chondrocytes, osteoblasts, and MSCs [23]. The functional RGD peptide is a cell adhesion motif, found in ECM proteins including fibronectin (FN) [24] and suggested to positively contribute to the chondrogenesis of MSCs, although, the effect is controversial and dependent on application [25]. FN has been denoted to initiate the cellular signalling of chondrocyte differentiation [26] and is critical in orchestration of the assembly of further ECM proteins including collagen [27]. Furthermore, the down-regulation of FN can alter cell morphology and shape resulting in reduced chondrogenic differentiation [28].

Cationic molecules such as transforming growth factor beta (TGF- β) display affinity towards the negatively charged alginate molecules by way of the Coulombic interaction and can be freed from alginate with slow kinetics [29]. In addition, the 12th–14th type III repeats of fibronectin (FN III12–14) bind to the TGF- β superfamily with high affinity [30]. The TGF- β superfamily is made up of three type of isoforms (TGF- β 1, TGF- β 2, and TGF- β 3); however, exclusively, TGF- β 1 and TGF- β 3 are relevant for stem cell chondrogenic differentiation [31, 32]. TGF- β 3 displays a higher chondrogenic promise as compared to TGF- β 1, leading to enhanced differentiation [33]. However, it remains unclear, if this TGF- β 3 enhanced differentiation is correlated with higher responsiveness for chondrocyte hypertrophy.

We have generated an innovative alginate-FN micron-sized subunit carrier for chondrogenesis—*chondrobags*. This novel system allows high-throughput fabrication of reproducible microgels with precise control over the density of embedded cells, shape and mono-dispersity. The chondrobags incorporate FN to immobilise growth factors and encapsulated cells while bypassing the diffusion limit for oxygen and nutrition given the chondrobag size. In addition, using pearl-lace interlinking hydrogel-based structures, chondrobags can be used for alternative microfluidic-based bioprinting [34]. The alginate-FN chondrobags presenting TGF- β 1 in solid phase provide a favourable chondrogenic microenvironment for specific differentiation of *in situ* cultured skeletal stem cells (SSCs) and human

articular chondrocytes (HACs), with implications therein for future tissue engineering applications.

2. Materials and methods

2.1. Human bone marrow derived SSCs isolation and culture

Bone marrow was sourced from a patient undertaking total hip replacement surgery at Spire Hospital in conjunction with the full ethical consent and approval from the hospital ethics committee (LREC 194/99/w, 27/10/10), through which informed patient consent was attained. All procedures making use of human tissue and cells were carried out in agreement with stipulated recommendations and regulations. Bone marrow (male 70 years of age) was acquired and used for isolating and culturing human bone marrow derived SSCs as previously detailed [35]. Washed bone marrow mixture was sieved through a 70 μm cell filter and separated using Lymphoprep™ (Lonza). Prior to a wash step with magnetic activated cell sorting (MACS) buffer (BSA and EDTA in PBS), harvested mononuclear cells were incubated in blocking buffer (α -MEM, 10% human serum, 5% fetal calf serum (FCS) and 10 mg ml^{-1} bovine serum albumin). Cells were incubated in 1 ml of hybridoma-based STRO-1 antibody and following a wash with MACS buffer were re-suspended in 1 ml containing 800 μl MACs buffer and 200 μl rat anti-mouse IgM microbeads (Miltenyi Biotec Ltd). A second MACS harvest for target cells was followed by washing with MACS buffer. Isolated target cells were washed and re-suspended in α -MEM containing 10% FCS and 1% penicillin/streptomycin (P/S) and cultured in tissue culture flasks.

2.2. Human articular chondrocytes isolation and culture

Femoral head was acquired from a male patient (61 years of age) undergoing total hip replacement surgery at Southampton General Hospital, in conjunction with the full ethical consent and approval from the hospital ethics committee (LREC 194/99/w, 27/10/10), with informed patient consent attained. The OA femoral head was classified as end stage OA (3–5 OARSI). The articular cartilage was dissected from the femoral head and sliced into small sections within 6 h post-surgery. Cartilage sections were incubated for 30 min at 37 °C in 10% trypsin (Sigma Aldrich) followed by 15 min in 0.1% hyaluronidase (Sigma Aldrich) following a wash with PBS. This trypsin-hyaluronidase step was followed by a further wash and incubation for 12–15 h at 37 °C in 1% collagenase B (Roche Diagnostics). The suspension containing the digested articular chondrocytes was filtered through a 70 μm filter. Isolated chondrocytes were re-suspended in DMEM/F12 containing 5% FCS, 1% insulin-transferrin-selenium (ITS) (Sigma-Aldrich), 1% P/S and 0.2% of ascorbic

acid (Sigma-Aldrich), and placed into tissue culture flasks.

2.3. Microfluidic fabrication

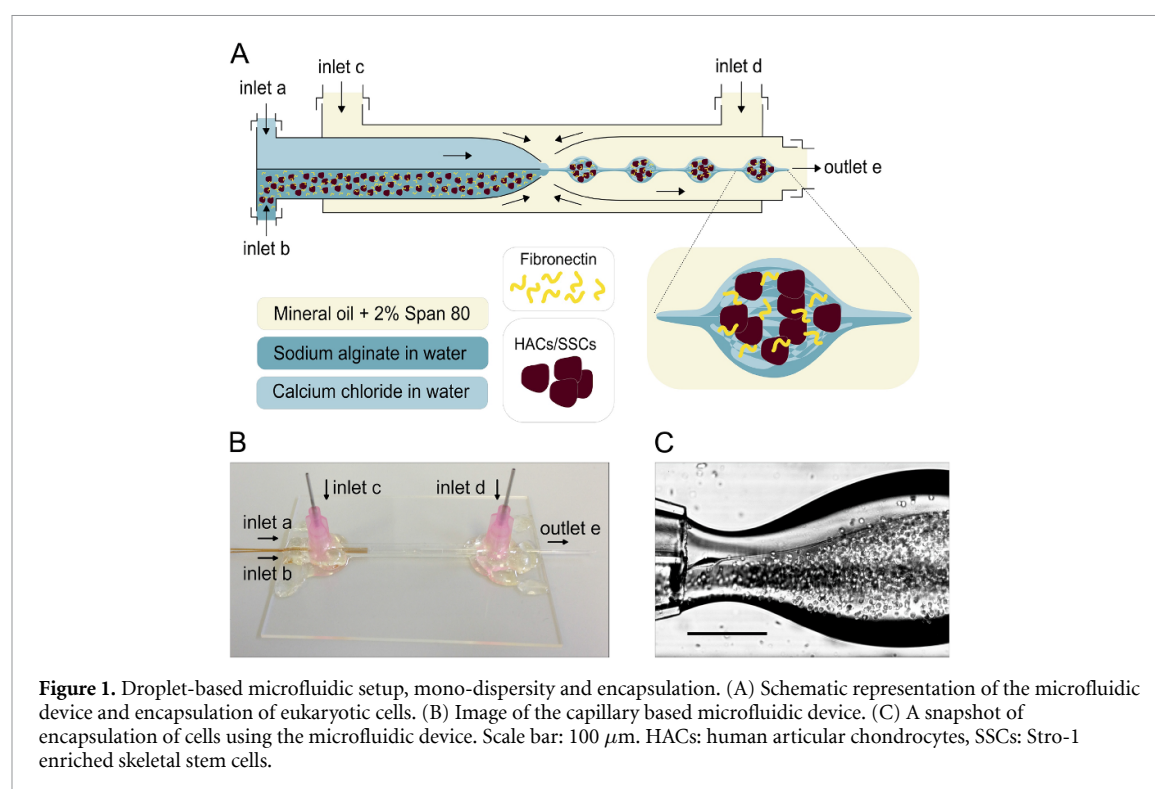
Co-flow focusing glass capillary device (figures 1(A) and (B)) for pearl-lace like microgel production developed in this study, was first reported by Witte *et al* [34]. Glass capillaries (<1.8 mm, TST150-6 and TW100-6, World precision instruments, Inc.) were tapered to desired hole sizes (0.04–0.07 mm) using a micropipette puller (P-97, Sutter Instruments) and centrally aligned in a square capillary of 2 mm ID (World precision instruments, Inc.). Sigmacote (Sigma-Aldrich) was used to modify the glass surface generating a hydrophobic layer. Capillaries were fixed on a cover-slide and using soft tubing, coupled with controllable syringe pumps (Harvard Apparatus).

2.4. Cell encapsulation

Both SSCs and HACs populations were initially treated for 40 min with collagenase IV (200 $\mu\text{g ml}^{-1}$) in α -MEM prior to detachment from culture plates using 0.025% (w/v) Trypsin–EDTA with 0.05% glucose for 10 min at 37 °C. To prepare a 2% alginate mixture, both cell types were individually re-suspended in the corresponding basal media and subsequently mixed 1:1 together with a medium viscosity 4% (w/v) sodium alginate (Sigma-Aldrich, UK) solution. FN sourced from human plasma (Sigma) was added to the mixture to give a final concentration 20 $\mu\text{g ml}^{-1}$. The water-based alginic cell mixture entered the microfluidic device through one of the two channels of a theta-shaped capillary, while leaving the other channel for 200 mM calcium chloride aqueous solution. Mineral oil (Sigma-Aldrich, UK) with 2% Span 80 (Sigma-Aldrich, UK) was introduced as the continuous phase through a square-shaped housing capillary for dispersing the two water-based solutions as they mixed within the flow focusing regime. Pre-warmed basal culture media was used as the collection solution for formed hydrogels. This step was followed by a 100 mM calcium chloride wash before culturing in either basal media or chondrogenic media comprising 10 nM dexamethasone, 100 μM ascorbic acid, 10 $\mu\text{g ml}^{-1}$ ITS and 10 ng ml^{-1} of either TGF- β 1 or TGF- β 3 (Peprotech) at 37 °C and 5% CO₂ in a humidified atmosphere. Media (chondrogenic differentiation media and basal media) was changed every 2 days until the end of the experiment at day 28.

2.5. Viability assay

Viability studies were carried out following incubation of the cell-laden hydrogels for an hour at 37 °C in a 100 mM calcium chloride solution containing 2 μM calcein and 2 μM ethidium homodimer-1 (EthD-1) (Viability/Cytotoxicity Kit, Life Technologies, UK). For the viability calculation, the total number of live cells (stained green) were analysed in comparison to



the total number of cells (stained either green or red). Viability was expressed as a percentage of the control. The hardware and software from EVOS Fl Colour Cell Imaging System were used for assigning the stained samples (green for live and red for dead cells). For measuring the pixel intensity of the fluorescence signals, sample images were processed using ImageJ software version 1.51 (100) and later graphed using GraphPad Prism (version 8.0 software).

2.6. RNA isolation and quantification

Chondrobags were prepared with a PBS wash at the end of the culturing period, prior to a 10 min incubation at 37 °C incubation with 1 ml of dissolving buffer (0.055 M sodium citrate, in 0.03 M EDTA, 0.15 M NaCl, pH 6.8) at 1000 rpm. This step was followed by centrifugation at 10 000 rpm for 2 minutes, a PBS wash and another round of centrifugation at 14 500 rpm for two minutes. 350 ml of RLT Plus Buffer was used to lyse the pellets formed by the cells. The lysed cell mixture was added to 540 ml RNA-free water and 10 ml Protease K solution (Qiagen) and further incubated for 10 min at 1000 rpm, 55 °C. AllPrep DNA/RNA/miRNA Universal Kit (Qiagen) was used to isolate RNA from the samples following the guidelines by the manufacturer. Extracted RNA samples were quantified using a Nanodrop ND-1000 spectrophotometer.

2.7. cDNA synthesis and mRNA expression analysis

cDNA synthesis and real time quantitative PCR (qPCR) were carried out to analyse expression of mRNA in human SSCs and HACs. SuperScript® VILO cDNA Synthesis kit from Applied Biosystems was

used for the synthesis of cDNA from sample containing isolated RNA. In brief, RNA was mixed with 2 μl 5X VILO™ reaction mix and 1 μl 10X SuperScript® enzyme. The mixture was subsequently incubated for 10 min at 25 °C and, thereafter, by a further incubation at 42 °C for 2 h and 85 °C for 5 min. qPCR was carried out with 10 μl of GoTaq master mix (Promega), 5 μl of upH₂O and 2 μl of reverse primer and 2 μl of forward primer for the gene of interest (primers listed in table S1) and 1 μl of sample containing isolated RNA. A 96 well-plate with each well containing a final mixture of 20 μl was later analysed using Applied Biosystems, 7500 Real Time PCR system. Acquired data was analysed using version 2.0.5 program of Applied Biosystems 7500 System SDS. To identify the most stable housekeeping genes, standard optimisation procedures were performed. For normalising Ct (cross-over threshold) values for SSCs experiments, *ACTB* as the endogenous housekeeping gene and for HACs analysis, *GAPDH* were used respectively. The fold expression levels were calculated using delta-delta Ct method for each target gene. All the sample readouts as well as control (negative control with no cDNA) were analysed from triplicates.

2.8. miRNA expression analysis

RNA extracted as detailed in *RNA isolation and quantification* were assessed for expression of: miR-140, miR-146b or miR-138 using TaqMan® MiRNA Assays (Table S2). Every individual assay contained two primers: one primer was used for cDNA synthesis and the second primer was used to perform

TaqMan q-PCR. For generating cDNA specific to each individual assay, specific miRNA from total RNA was generated with TaqMan® MiRNA Reverse Transcription Kit using a modified protocol from the manufacturer. In brief, a reaction mixture containing of 3.58 μl upH₂O, 0.75 μl 10X Buffer, 1.88 μl of RNase inhibitor, 1.50 μl of RT primer, 0.08 μl of dNTPs and 10 ng of total RNA was made and incubated at 16 °C for 30 min followed by 30 min at 42 °C and further 5 min of incubation at 85 °C before termination at 42 °C. qPCR was carried out with 5 μl of TaqMan® Universal PCR Master Mix containing No AmpErase® UNG from Life technologies. The qPCR also included 3.34 μl of upH₂O, 0.5 μl of TM primer and 0.8 μl of cDNA. A 96 well-plate containing this mixture was assessed using Applied Biosystems, 7500 Real Time PCR system and data gathered analysed using version 2.0.5 program from Applied Biosystems 7500 System SDS. Standard optimisation procedures were performed to determine the appropriate housekeeping gene for the study of miRNA expression. For normalising Ct values, RNU44, was used as a housekeeping control RNA for miRNA. To calculate the fold expression level of each gene of interest, delta-delta Ct method was employed. All sample readouts, including negative controls (no cDNA), were analysed from duplicates.

2.9. Enzyme linked immunosorbent assay (ELISA)

Solid Phase Sandwich ELISA for transforming Growth Factor Beta 1 and 3 release from the alginate construct were measured using Human TGF- β 1 DuoSet ELISA (DY240-05) and Human TGF- β 3 DuoSet ELISA (DY243) kits from R&D systems. 0.5 ml of alginate micro-beads (with and without FN at 20 $\mu\text{g ml}^{-1}$ concentration) were soaked in 5 ml DMEM media containing either TGF- β 1 or TGF- β 3 at the concentration of 10 ng ml⁻¹ overnight. The following day, micro-beads were placed into fresh media and samples for ELISA were taken at 1.5, 3, 6 and 24 h. ELISA steps were carried out according to manufacturer's instructions and the readouts performed using BioTek™ Synergy™ HT Multi-Detection Microplate Reader.

2.10. Histology

Chondroblasts were washed in 0.1 mM calcium chloride and fixed in 10% buffered formalin (neutral) prior to histological analysis. Specimens were dried using a series of graded ethanols, embedded in OCT (Cell-Path, UK) and cryo-sectioned at 5 μm thickness. Dehydrated sections were collected onto APEs coated slides, air dried for 30 min and stored at -20 °C until required for staining. For histological evaluation, sections were warmed at 37 °C for 30 min and washed in RO water prior to staining with Alcian Blue/Sirius Red and Safranin O/Fast Green. Briefly, sections were stained with Weigert's haematoxylin (A and B, 1:1 mix, Clin-Tech, UK) for 10 min prior to staining

with 0.5% Alcian Blue (Sigma, UK) for 10 min, followed with molybdophosphoric acid (Sigma, UK) for 10 min and finally with Sirius Red (Clin-Tech, UK) for an hour or were stained with Fast Green (FCF) solution for 5 min followed with Safranin O for 5 min. Between each staining step, slides were rinsed in a water bath for 1 min and drained. Slides were finally dehydrated through increasing ethanol concentrations and cleared in HistoClear (50%, 90%, 100%-1, 100%-2 ethanol and HistoClear-1 and 2 each for 30 s) before being mounted in p-xylene bis-pyridinium bromide (DPX). Sections were observed using an Olympus dotSlide Virtual Microscopy System and images processed using Olympus OlyVIA 2.9 image analysis software.

2.11. Statistical analysis

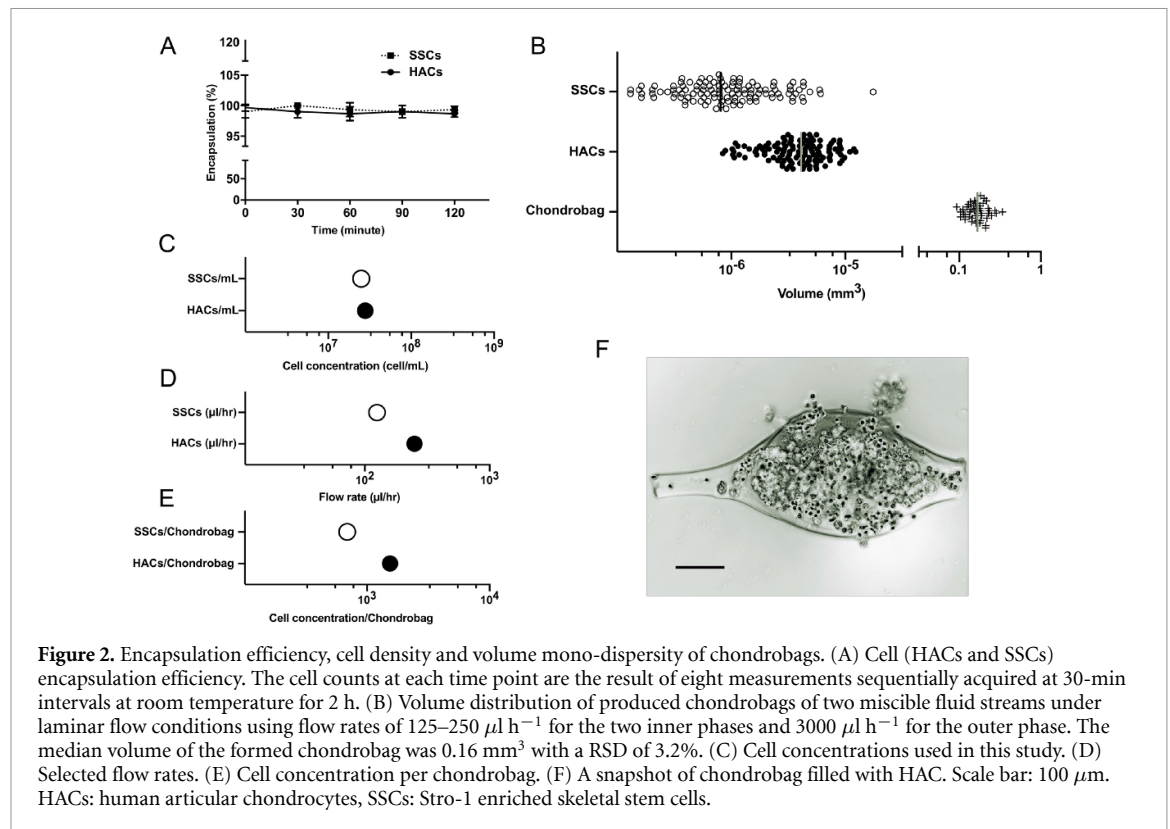
Data are presented as mean values and standard deviations (SD). Statistical analysis was performed by a one-way ANOVA, a Tukey post-hoc test and Student's *t* test in GraphPad Prism™ 8 software with a level of significance of $p < 0.1$ marked by *, $p < 0.05$ marked by **, $p < 0.001$ marked by *** and $p < 0.0001$ marked by ****.

3. Results and discussion

3.1. Microfluidic fabrication of mono-dispersed alginate-fibronectin chondroblasts and encapsulation of SSCs and HACs

SSCs and HACs were encapsulated in pearl-lace like chondroblasts using co-flow focusing glass capillary devices (figures 1(A)–(C) and supplementary video 1 and 2 (available online at <https://stacks.iop.org/BF/12/045034/mmedia>)). The design was optimised in respect to our previous report for encapsulation of a co-culture of MSCs and engineered bacteria [34].

The alginate-calcium composite is a diffusion-based hydrogel prepared by ionic cross-linking. Diffusion is a time-dependent process and for this reason, fully homogeneous hydrogels can never be fully attained. Nevertheless, as the bead size is reduced, heterogeneity is reduced between formed hydrogels. As a consequence, calcium diffusion occurred rapidly in the micro-sized beads leading to improved and high encapsulation efficiency (>99%) (figure 2(A)) within each microgel (supplementary Video 2), leading to the generation of reproducible chondroblasts (figure 2(B)). The shape and size of the pearl-lace microgel construct chosen for this study provided efficient volume ratios between material and cell, eliminating the diffusion cap of 100 to 200 μm for the transport of oxygen, nutrients including ingress of vital biomolecules for encapsulated cells and facilitation of removal of cell waste [36]. Chondroblasts were generated at 5–10 units per second within selected flow rates containing $\sim 2.6 \times 10^7$ cells ml⁻¹ (figures 2(C) and



(D)). This resulted in cells residing in close proximity ($\sim 10^3$ cells per chondrobag, figure 2(E)) while facilitating nutrition and waste diffusing through the porous micro-structures of the alginate-FN hydrogel (figure 2(F)).

The superiority of 3D over 2D cultures to enhance stem cells functions are well documented, and the culture of SSCs in 3D has previously demonstrated enhanced stromal differentiation along the chondrogenic lineage [37]. In contrast to 2D cultures, the culture of stem cells in 3D promoted enhanced cell-cell contact; facilitating exposure of cells to substrates with different physical properties including viscoelasticity and topography together with the display of assorted endogenous and exogenous ECM adhesion motifs for integrins [37]. The application of droplet microfluidics for 3D micromass formation with HACs and SSCs, together with *in situ* fine temporal control over the constituents of biomaterials provided a powerful platform to deliver reproducible and, crucially, a high-throughput formation of functional micromass constructs [38, 39]. Such a strategy has been undertaken using pluripotent stem cells [40–42]. The incorporation of mechanical stress [43] and hypoxia [44], offer future approaches to enhance and further mimic the physiological environment to enhance chondrogenic differentiation.

It has been shown that a bone-like physicochemical microenvironment can override chondroinductive signals including TGF- β 1. The extracellular calcium-sensing receptor (CaSR)

of human BM-derived MSCs has shown to become hyperstimulated by bone-like biomimetic hydroxyapatite (BBHAp) [45]. However, in this study, the calcium concentration used to gel the alginate acid was retained at the same level for all samples including the negative control constructs while studying the impact of TGF- β 1 and TGF- β 3 separately in FN containing chondrobags.

Studies have established that the permeable structure of a scaffold can aid cell attachment, proliferation and differentiation, which can lead to generation of the phenotype of interest in a cell [32, 46]. Chondrobags combine alginate and FN to provide a cost-effective facile strategy for three-dimensional construct generation (18–36 k chondrobags per hour) with a clear potential for cartilage tissue engineering. Correct porosity provides appropriate shape and environmental cues through mimicry of the chondrocyte lacunae to facilitate proliferation and differentiation. The favourable porosity, thin walls and excellent interconnectivity between pores of the hydrogel, contribute to nutrient and metabolic waste exchange. The induced condensation of HACs and SSCs in chondrobags is a significant milestone in comparison to current conventional scaffold-free systems requiring 3D culture, predominantly based on micromass pellets derived using centrifugation [8]. The use of centrifugation, as an initial step, typically generates restrictive cell to cell and cell to ECM interactions, resulting in high variability in the time required to form 3D aggregates [9]. In addition,

traditional macro-pellet models are often too large and, typically, suffer from heterogeneity of cell phenotype and the formation of necrotic cores [8, 47]. As shown in Supplementary Video 3, pearl-on-thread chondrobags can be used as a low-cost cell-laden bioprinting alternative.

3.2. Skeletal cell viability, cell cluster and micro-mass formation in chondrobags

The advantages of reduced shear stress experienced during cell encapsulation in chondrobags due to the channel design and low flow rates of this micro-fluidic design [34], contributed to high cell viability observed throughout the hydrogel. Evaluation of the cell viability of HACs and SSCs demonstrated the presence of live cells (>90%) with negligible necrotic cells present in the central regions of cell clusters in the chondrobags. Viability and biocompatibility of alginate-FN chondrobags was confirmed 1, 3 and 24 h following encapsulation and, crucially, at the conclusion of the studies, on day 28. Figures 3(A)–(D) demonstrate the level of viability observed following encapsulation at day 0 and at 28 d. For HACs, no differences in cell viability were observed between cells cultured in chondrogenic media with TGF- β 1 or TGF- β 3 (figures 3(A) and (B)). Enhanced HACs cell numbers were observed within chondrobags loaded with TGF- β 3 with an average of 11.8 cells per cluster, as compared to 8.3 cells per cluster in TGF- β 1 and 1.8 cells per cluster for control samples (figure 3(H)). This variation is likely a consequence of differences in cell proliferation, given all the samples comprised the same initial cell density per chondrobag (figure 2(E)). In addition to higher cell counts per cluster (1.4 times), the area of clusters in TGF- β 3 was almost twice (1.9 times, normalised against area of cell clusters in control sample) the size as compared to those stimulated with TGF- β 1 (figure 3(G)). Interestingly, this finding is consistent with the cell volume expansion of hypertrophic chondrocytes in the growth plate, as a consequence of an increase in organelles and increased metabolic activity [48]. Mueller and collaborators have reported this to be the case for the enhancement of hypertrophy in MSC chondrogenesis [49].

SSCs encapsulated within chondrobags displayed a discrete increase in the numbers of necrotic cells following stimulation with TGF- β 3 and TGF- β 1, as compared to the control samples (figures 3(C) and (D)). The micromass samples generated by SSCs within chondrobags, stimulated with TGF- β 1 or TGF- β 3, were noted to be more compact with no clear border (space) between cells within the same cluster/colony (figures 3(C) and (F)) as compared to the more dispersed HACs micromass samples (figures 3(A) and (E)) after 28 d. The slight rise in the total number of necrotic cells in the centre of SSCs micromass samples is likely due, in part, to the larger

size of the compact cell masses due to cell proliferation (7 and 5.1 times larger cluster area, normalised against area of cell clusters, in control sample for TGF- β 1 and TGF- β 3, respectively. Figure 3(G)). Hence, hypoxia may have been induced with cells at the centre of the compact mass potentially deprived of nutrients/oxygen. These observations are significant given current literature has evidenced viability but limited cell proliferation [21].

3.3. Quantification of TGF- β in chondrobags

FN is known to have specific interactions with a diverse range of GFs, such as PDGF, FGF, IGF, TGF- β and others [30, 50]. The extent of this interaction varies within members of each superfamily. Within the TGF- β superfamily, TGF- β 1, BMP-2, and BMP-7 display a high measure of affinity to a domain containing the 12th to 14th type III copies of FN (FN III12–14). However, in comparison, TGF- β 2, TGF- β 3, BMP-4, and BMP-6 did not exhibit notable binding to FN [30]. Consistent with this finding, GF release studies in chondrobags demonstrated that alginate-FN microgels display a 4-fold higher affinity for TGF- β 1 in comparison to TGF- β 3 (figure 4). TGF- β 1 was loaded and observed to be slowly released over 24 h in alginate-FN hydrogels. In contrast, there was negligible release (and subsequent uptake) of TGF- β 1 in alginate-based chondrobags, in the absence of FN. The same conditions examined for TGF- β 3 in FN-free chondrobags resulted in no detectable readings (figure 4). TGF- β 1 and TGF- β 3 interactions with FN result in modulation of their parting from the alginate-FN microgel (solid phase) to the soluble phase, hence regulating their diffusion, and dissipation concentration locally and consequently influencing cell signalling. We showed that higher local concentrations of TGF- β 1 in chondrobags are influenced by the presence of FN. We hypothesise that TGF- β 1 is bound to FN (FNIII12–14) and, given this occurs adjacent to the integrin binding region (FNIII9–10), provides the alginate-FN microgels with synergistic TGF- β 1/integrin signalling leading into a highly permissive chondrogenic microenvironment [51] (figure 2(F)).

3.4. Quantification of gene expression in HACs and SSCs cultured chondrobags

qPCR of chondrocyte-related marker transcripts was used to demonstrate the chondrogenic differentiation of SSCs (figures 5(K)–(T)) and the phenotype maintenance of HACs (figures 5(A)–(J)), following encapsulation within engineered alginate-FN chondrobags, with growth factors bound to FN and presented from a solid phase. The chondrogenic gene *SOX9* has been observed during the *in vitro* induction of chondrogenesis and the subsequent promotion of the transcription of cartilage proteins, including

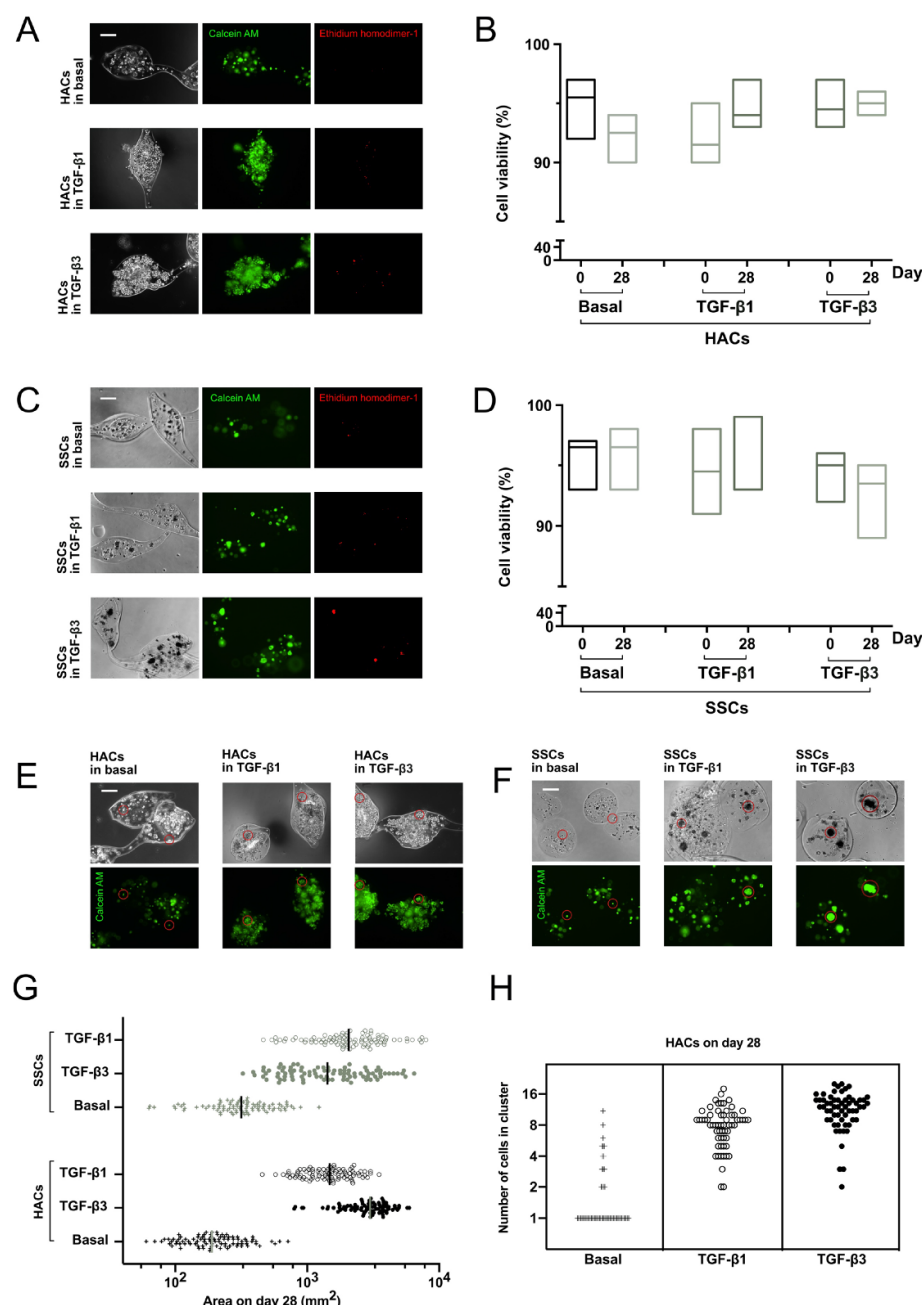
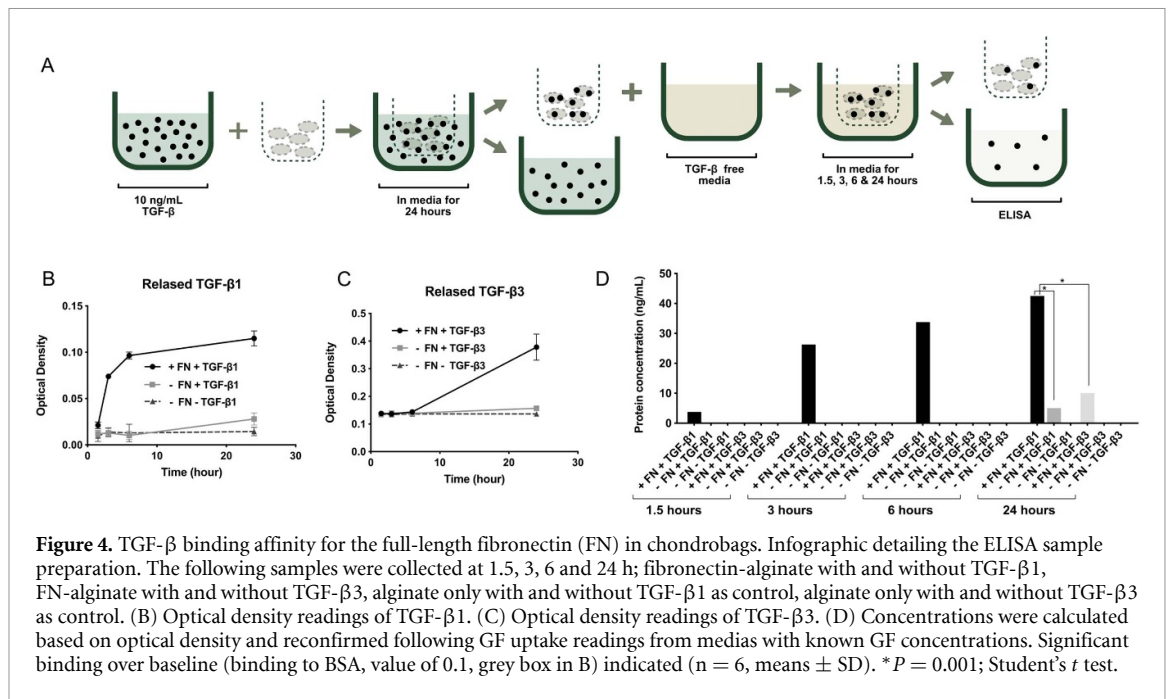


Figure 3. Skeletal cell viability, cell cluster and micro-mass formation in chondroblasts. (A) Microscopy images of alginate-fibronectin (FN) chondroblasts containing human articular chondrocytes (HACs) cultured in the presence of TGF-β1 or TGF-β3 for up to 28 d relative to untreated control. (B) HACs viability graph. (C) Microscopy images of alginate-FN chondroblasts containing Stro-1 enriched skeletal stem cells (SSCs) cultured in the presence of TGF-β1 or TGF-β3 for up to 28 d relative to untreated control. (D) SSCs viability graph. (E) Microscopy images of alginate-FN chondroblasts containing HACs cultured in the presence of TGF-β1 or TGF-β3 for up to 28 d relative to untreated basal control. Individual cells are highlighted within a red circle. (F) Microscopy images of alginate-FN chondroblasts containing SSCs cultured in the presence of TGF-β1 or TGF-β3 for up to 28 d relative to untreated basal control. Micro-masses are highlighted within a red circle. (G) Graph with area of SSCs and HACs cultured in the presence of TGF-β1 or TGF-β3 for up to 28 d relative to untreated basal control. (H) Graph with number of cells found in clusters containing HACs after 28 d. Cells in green are stained with Calcein AM. Scale bar: 100 μm. The hydrogel was stained with Viability/Cytotoxicity Kit with viable cells in green (Calcein AM) and non-viable cells in red (Ethidium homodimer-1). Scale bar: 100 μm. N ≥ 5–10 microgels were analysed for each condition. Additional images can be found in supplementary figure 1.

type II collagen and aggrecan [52]. Type II collagen (COL2A1) is the predominant collagen present in physiological hyaline cartilage, providing cartilage with tensile strength [53]. Aggrecan (ACAN), the characteristic proteoglycan produced by chondrocytes, has been shown to link to collagen fibrils via

hyaluronic acid. Importantly, the polyanionic nature of aggrecan draws water, which provides for cartilage expansion, key to the generation of mechanical function [54].

Expression of *SOX9* (early marker), *COL2A1* (mid/late marker) and *ACAN* confirmed the potential



of alginate-FN chondroblasts to maintain the chondrogenic phenotype of HACs. These markers showed no significant differences between chondroblasts loaded with either GFs; despite TGF- β 3 not being bound to chondroblasts with as high affinity as TGF- β 1 (figure 4). Chondrogenic associated *SOX9* expression was observed to be notably up-regulated in HACs loaded with TGF- β 1 (4.1-fold change) and loaded with TGF- β 3 (3.6-fold change) (figure 5(A)). This was also observed for *COL2A1*: with TGF- β 1 (111.4-fold change) and treated with TGF- β 3 (252.7-fold change) (figure 5(B)), and *ACAN*: 8.5-fold change with TGF- β 1 and 8.1-fold change treated with TGF- β 3 (figure 5(C)). This cumulative increase in the expression of *COL2A1* and *ACAN* was in line with previous studies [22, 55].

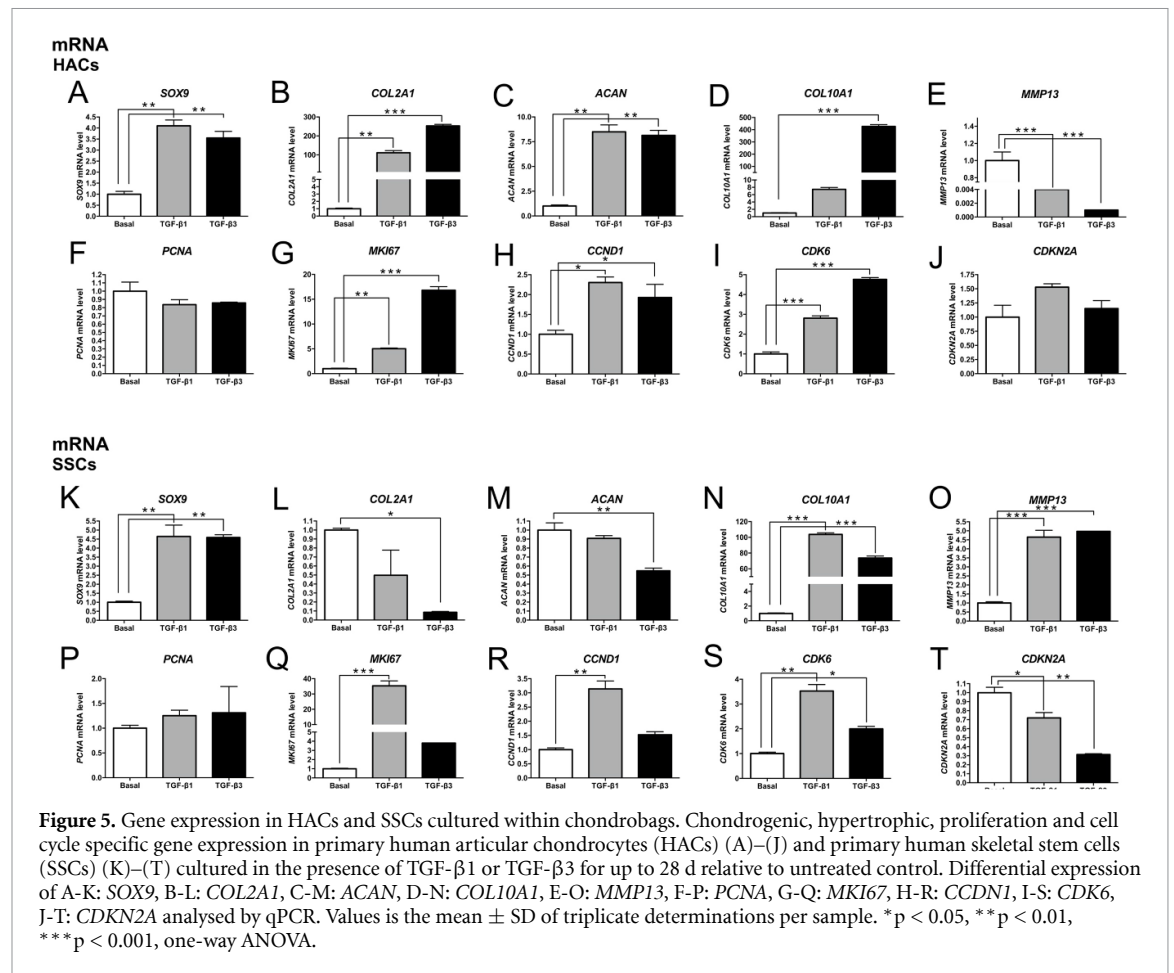
In contrast, SSCs did not display a clear and significant differentiation along the chondrogenic lineage. However, several studies have identified a discrete decrease in aggrecan expression for cells cultured within a 3D construct, supporting the current findings using SSCs (figure 5(M)). Only *SOX9* expression was significantly up-regulated following SSCs treatment with TGF- β 1 (4.7-fold change) and treatment with TGF- β 3 (4.6-fold change) (figure 5(K)).

There are a number of markers of hypertrophic chondrocytes, with collagen type X and MMP13 the most widely recognised [52, 56]. Type X collagen functions as a substructure for ensuing matrix calcification [57]. Hypertrophic ECM functionally differs to physiological hyaline cartilage and, in part, comparable to bone matrix. In this context, the current studies indicate that following 28 d of chondrogenic differentiation, HACs in chondroblasts with TGF- β 1 bound to FN displayed reduced commitment to

the formation of hypertrophic chondrocytes, compared to cells stimulated with TGF- β 3 (figures 5(D)–(E)). Strikingly, the current results observed using engineered chondroblasts, with TGF- β 1 bound to FN, demonstrate negligible evidence of hypertrophic chondrocytes, enabling the maintenance of the required chondrocytic phenotype for cartilage tissue repair.

Specific genes for proliferation and cell cycle [58] were also examined. HACs and SSCs encapsulation in alginate-FN chondroblasts resulted in modulation of essential components in G1/S, with decreased levels of p16 (*CDKN2A*), increased *CDK6* and cyclin expression (*CCDN1*), resulting in enhanced cell cycle progression and proliferation (figures 5(H)–(J) and (R)–(T)). In the current study, we observed a significant up-regulation of *MKI67* in cells encapsulated in chondroblasts with TGF- β 1 bound to FN (5-fold change for HACs and 35-fold change for SSCs) (figures 5(G) and (Q)) and to TGF- β 3 (1.9-fold change for HACs and 1.5-fold change for SSCs) (figures 5(G) and (Q)), indicating higher proliferative activity of cells within TGF- β 3 alginate-FN chondroblasts than cells within TGF- β 1.

TGF- β 1 appears to be closely connected with cell growth and differentiation providing a crucial role in the regulation of autocrine and paracrine processes [59]. In addition, TGF- β 1 is a growth modulator with multi-physiological potencies on immune suppression and inflammation, cell differentiation, wound healing and cancer [60]. However, Mueller and colleagues failed to detect any differences between aggregates preconditioned with TGF- β 1 and TGF- β 3 following histological evaluation and quantification of alkaline phosphatase (ALP) secretion [49].



The likely differences from our study reside with the observation that in the engineered chondrobags, TGF-β1 is also bound to FN and presented from a solid phase (figure 4), with TGF-β1 more accessible to the encapsulated cells and thus favouring chondrogenic differentiation.

3.5. microRNA profiling in HACs and SSCs cultured in chondrobags

Small noncoding RNAs (19–24 nucleotides long) have gained significant research interest in recent years [61]. MicroRNAs (miRNAs) in particular are important regulators of gene expression [62]. miRNAs are involved in the process of stem cell differentiation, together with stem cell therapy and can prompt skeletal regeneration and thus, miRNAs offer innovative approaches to prevent/treat OA and osteoporosis (OP) [63]. Following culture of HACs and SSCs with or without TGF-β1 or TGF-β3 for 28 d, TaqMan qPCR was used to determine the expression levels of miRNAs. miR-140 was employed as a positive control for chondrogenic differentiation [64]. Chondrogenic related miR-140-3p expression was notably up-regulated in the encapsulated cells in TGF-β1 alginate-FN chondrobags (61.8-fold change for HACs and 1.7-fold change for SSCs) (figures 6(A) and (D)) and TGF-β3 alginate-FN chondrobags (81.2-fold

change for HACs and 3.4-fold change for SSCs) (figures 6(A) and (D)). miR-140 is an important modulator of cartilage homeostasis and implicated in OA. Critically, miR-140 is almost uniquely and abundantly expressed in chondrocytes [65] and, in addition, plays an important role in bone development, at least in part by controlling proliferation. Miyaki and collaborators reported that throughout chondrogenesis, miR-140 expression levels increase in differentiated human MSCs in comparison to undifferentiated MSC populations together with expression of COL2A1, ACAN and SOX9. These findings indicate miR-140 is a marker and potential modulator of chondrogenesis [66].

In contrast, miR-146b expression was significantly down-regulated in cells encapsulated in TGF-β1 alginate-FN chondrobags (0.8-fold change for HACs and 0.1-fold change for SSCs) (figures 6(B) and (E)) and in TGF-β3 alginate-FN chondrobags (0.5-fold change for HACs and 0.2-fold change for SSCs) (figures 6(B) and (E)). Compared to chondrobags cultured in basal media, miR-146b was down-regulated during chondrogenic differentiation of human bone marrow derived SSCs. Furthermore, we have previously shown that miR-146b serves as a negative modulator of chondrogenesis, with an important role in the regulation of SOX5 expression

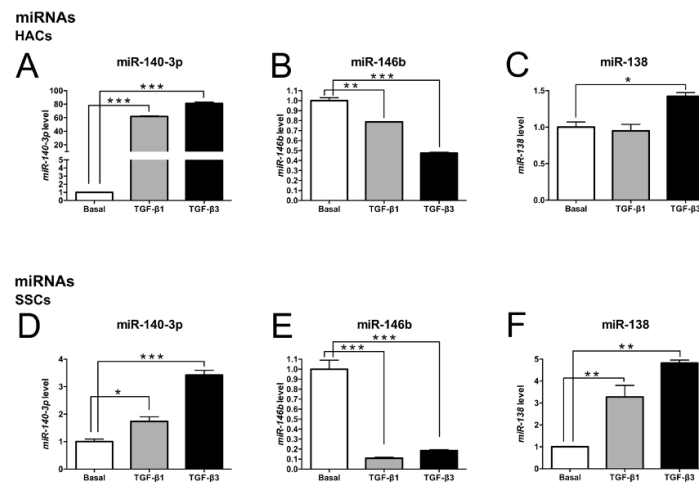


Figure 6. MicroRNA profiling in HACs and SSCs cultured within chondrobags. miRNA expression in primary human articular chondrocytes (HACs) (A-C) and primary human skeletal stem cells (SSCs) (D-F) cultured in the presence of TGF- β 1 or TGF- β 3 for up to 28 d relative to untreated control. Differential expression of A-D: miR-140, B-E: miR-146b, C-F: miR-138, analysed by TaqMan qPCR. Values represent mean \pm SD of duplicate determinations per sample. * $p < 0.05$, ** $p < 0.01$, *** $p < 0.001$, one-way ANOVA.

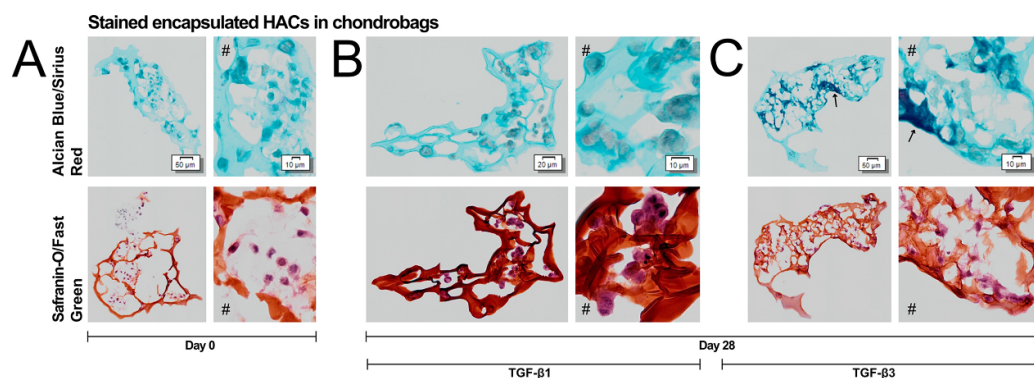


Figure 7. Stained encapsulated human articular chondrocytes (HACs) in alginate-fibronectin chondrobags. Alcian Blue/Sirius Red (top row) and Safranin O/Fast Green-stained (bottom row) histological sections of chondrocytes-laden chondrobags (5 μ m sections). Histological appearance of chondrobags following basal culture for day 0 (A) and day 28 cultured in the presence of TGF- β 1 (B) and day 28 cultured in the presence of TGF- β 3 (C). All images accompanied with larger magnification (right images, #). Arrows are pointing to darker Alcian Blue staining as compared to the background lighter blue stain.

during the chondrogenic differentiation of human bone marrow derived SSCs [67].

miR-138 expression was observed to be notably up-regulated in HACs encapsulated in TGF- β 3 alginate-FN chondrobags (1.4-fold change) but not with TGF- β 1 (0.95-fold change) (figure 6(C)). miR-138 expression in SSCs was significantly up-regulated under both conditions: 3.3-fold change with TGF- β 1 and 4.8-fold change with TGF- β 3 (figure 6(F)). These results demonstrate the commitment of HACs and SSCs following culture for 28 d in the chondrobags towards the chondrogenic lineage. The overexpression of miR-138 has been shown to inhibit osteoblast differentiation hMSCs *in vitro*. miR-138 inhibition serves as an anti-miR-138 for promoting expression of osteoblast-specific genes as well as the activity of ALP and matrix mineralization [68].

3.6. Histological analysis of collagen formation in chondrobags

Chondrobags encapsulating HACs cultured *in vitro* for 28 d in the presence of TGF- β 1 or TGF- β 3 indicated enhanced cell proliferation evidenced by increased collagen deposits with faint Sirius Red staining compared to control (figure 7). This result correlated with the observation of growth and proliferation observed in figure 3 as well as gene expression results for proliferation and cell cycle markers in figures 5(F)–(J)). In contrast, intense Alcian Blue staining (but not Sirius Red staining) was observed in the matrix of chondrobags cultured in the presence of TGF- β 3 (figure 7(C)) as compared to TGF- β 1 (figure 7(B)) indicating the formation of ECM (arrow). The comparatively intensive Alcian Blue staining of cartilage matrix and proteoglycans in chondrobags cultured in presence

of TGF- β 3 correlated with the observed gene expression studies of collagen II (*COL2A1*, figure 5(B)) and collagen X (*COL10A1*, figure 5(D)) from similarly treated samples. Safranin-O stains polyanions in alginate [69], thus, the formation of new cartilage in the chondrobags can be difficult to determine. Nevertheless, the distribution of nuclei within the chondrobags can be clearly observed (figure 7). The lack of fast green staining observed confirmed the absence of bone formation within these sections.

4. Conclusion

The current findings demonstrate that engineered TGF- β 1 alginate-FN chondrobags provide an appropriate biomimetic environment for the formation of hyaline cartilage *in vitro*. We demonstrate that TGF- β 1 bound to FN and presented from a solid phase, facilitates and enhances chondrogenic differentiation. Importantly, TGF- β 1 loaded chondrobags promote chondrogenesis without the formation of hypertrophic chondrocytes. This cue-integrated-3D biomaterial platform, demonstrated increased proliferation, enhanced cell viability, chondrogenic differentiation of SSCs *in situ* and phenotype maintenance for HACs. The current studies illustrate the potential applications for a TGF- β 1 alginate-FN chondrobags platform as a workable 3D bioprinting and culture system for cartilage tissue regeneration with therapeutic applications therein.

Acknowledgments

The support from the UK Engineering and Physical Sciences Research Council (Grant No: EP/P001114/1) is acknowledged as well as support from the UK Regenerative Medicine Platform Hub Acellular SMART materials 3D architecture (Grant No: MR/R015651/1) and a grant from the UK Regenerative Medicine Platform (Grant No: MR/L012626/1 Southampton Imaging) is gratefully acknowledged. We thank Jon Ward and Carol Ann Smith for technical support.

Author contributions

The manuscript was written through contributions from all authors. All authors have given approval to the final version of the manuscript. The authors, Kimia Witte and María C. de Andrés contributed equally.

Notes

The authors declare no competing financial interest.

All the original data related to this article are within the depository of the University of Glasgow (<http://dx.doi.org/10.5525/gla.researchdata.871>).

ORCID iDs

Kimia Witte

<https://orcid.org/0000-0003-4708-1621>

María C de Andrés

<https://orcid.org/0000-0003-2260-6356>

Julia Wells

<https://orcid.org/0000-0001-8272-0236>

Matthew J Dalby

<https://orcid.org/0000-0002-0528-3359>

Manuel Salmeron-Sanchez

<https://orcid.org/0000-0002-8112-2100>

Richard O C Oreffo

<https://orcid.org/0000-0001-5995-6726>

References

- [1] Moradi L, Vasei M, Dehghan M M, Majidi M, Farzad Mohajeri S and Bonakdar S 2017 Regeneration of meniscus tissue using adipose mesenchymal stem cells-chondrocytes co-culture on a hybrid scaffold: In vivo study *Biomaterials* **126** 18
- [2] Kock L, van Donkelaar C C and Ito K 2012 Tissue engineering of functional articular cartilage: the current status *Cell Tissue Res.* **347** 613
- [3] Hunter D J and Felson D T 2006 Osteoarthritis *BMJ* **332** 639
- [4] Otto I A, Levato R, Webb W R, Khan I M, Breugem C C and Malda J 2018 Progenitor cells in auricular cartilage demonstrate cartilage-forming capacity in 3D hydrogel culture *Eur. Cell Mater.* **35** 132
- [5] Schulze-Tanzil G, de Souza P, Villegas Castrejon H, John T, Merker H J, Scheid A and M. S 2002 Redifferentiation of dedifferentiated human chondrocytes in high-density cultures *Cell Tissue Res.* **308** 371
- [6] Freyria A M, Yang Y, Chajra H, Rousseau C F, Ronziere M C, Herbage D and Haj A J E 2005 Optimization of dynamic culture conditions: Effects on biosynthetic activities of chondrocytes grown in collagen sponges *Tissue Eng.* **11** 674
- [7] Jukes J M, Moroni L, van Blitterswijk C A and de Boer J 2008 Critical steps toward a tissue-engineered cartilage implant using embryonic stem cells *Tissue Eng. A* **14** 135
- [8] Centola M, Tonnarelli B, Scharen S, Glaser N, Barbero A and Martin I 2013 Priming 3D cultures of human mesenchymal stromal cells toward cartilage formation via developmental pathways *Stem Cells Dev.* **22** 2849
- [9] Occhetta P, Centola M, Tonnarelli B, Redaelli A, Martin I and Rasponi M 2015 High-throughput microfluidic platform for 3D cultures of mesenchymal stem cells, towards engineering developmental processes *Sci Rep.* **5** 10288
- [10] Babur B K, Futrega K, Lott W B, Klein T J, Cooper-White J and Doran M R 2015 High-throughput bone and cartilage micropellet manufacture, followed by assembly of micropellets into biphasic osteochondral tissue *Cell Tissue Res.* **361** 755
- [11] Li F, Levinson C, Truong V X, Laurent-Applegate L A, Maniura-Weber K, Thissen H, Forsythe J S, Zenobi-Wong M and Frith J E 2020 Microencapsulation improves chondrogenesis in vitro and cartilaginous matrix stability in vivo compared to bulk encapsulation *Biomater. Sci.* **8** 1711
- [12] Nie M and Takeuchi S 2018 Bottom-up biofabrication using microfluidic techniques *Biofabrication* **10** 044103
- [13] Swieszkowski W, Dokmeci M R and Khademhosseini A 2020 Microfluidics in biofabrication *Biofabrication* **12** 030201
- [14] Tare R S, Babister J C, Kanczler J and Oreffo R O 2008 Skeletal stem cells: phenotype, biology and environmental niches informing tissue regeneration *Mol. Cell. Endocrinol.* **288** 11
- [15] Freyria A M, Ronziere M C, Cortial D, Galois L, Hartmann D, Herbage D and Mallein-Gerin F 2009

- Comparative phenotypic analysis of articular chondrocytes cultured within type I or type II collagen scaffolds *Tissue Eng. A* **15** 1233
- [16] Hwang N S, Varghese S, Zhang Z and Elisseeff J 2006 Chondrogenic differentiation of human embryonic stem cell-derived cells in arginine-glycine-aspartate-modified hydrogels *Tissue Eng.* **12** 2695
 - [17] Hwang N S, Varghese S and Elisseeff J 2007 *Cartilage Tissue Engineering* (Totowa, NJ: Humana Press)
 - [18] Luca G *et al* 2007 Encapsulation, in vitro characterization, and in vivo biocompatibility of Sertoli cells in alginate-based microcapsules *Tissue Eng.* **13** 641
 - [19] Ma H L, Hung S C, Lin S Y, Chen Y L and Lo W H 2003 Chondrogenesis of human mesenchymal stem cells encapsulated in alginate beads *J. Biomed. Mater. Res. A* **64** 273
 - [20] Tritz-Schiavi J *et al* 2010 Original approach for cartilage tissue engineering with mesenchymal stem cells *Biomed. Mater. Eng.* **20** 167
 - [21] Babister J C, Tare R S, Green D W, Inglis S, Mann S and Oreffo R O 2008 Genetic manipulation of human mesenchymal progenitors to promote chondrogenesis using "bead-in-bead" polysaccharide capsules *Biomaterials* **29** 58
 - [22] Park M H, Subbiah R, Kwon M J, Kim W J, Kim S H, Park K and Lee K 2018 The three dimensional cues-integrated-biomaterial potentiates differentiation of human mesenchymal stem cells *Carbohydr. Polym.* **202** 488
 - [23] Degala S, Zipfel W R and Bonassar L J 2011 Chondrocyte calcium signaling in response to fluid flow is regulated by matrix adhesion in 3-D alginate scaffolds *Arch. Biochem. Biophys.* **505** 112
 - [24] Mauck R L, Byers B A, Yuan X and Tuan R S 2007 Regulation of cartilaginous ECM gene transcription by chondrocytes and MSCs in 3D culture in response to dynamic loading *Biomech. Model Mechanobiol.* **6** 113
 - [25] Salinas C N and Anseth K S 2008 The enhancement of chondrogenic differentiation of human mesenchymal stem cells by enzymatically regulated RGD functionalities *Biomaterials* **29** 2370
 - [26] Tavella S *et al* 1997 Regulated expression of fibronectin, laminin and related integrin receptors during the early chondrocyte differentiation *J. Cell. Sci.* **110** 2261
 - [27] Sottile J and Hocking D C 2002 Fibronectin polymerization regulates the composition and stability of extracellular matrix fibrils and cell-matrix adhesions *Mol. Biol. Cell* **13** 3546
 - [28] DeLise A M, Fischer L and Tuan R S 2000 Cellular interactions and signaling in cartilage development *Osteoarthr. Cartil.* **8** 309
 - [29] Puolakkainen P A, Ranchalis J E, Gombotz W R, Hoffman A S, Mumper R J and Twardzik D R 1994 Novel delivery system for inducing quiescence in intestinal stem cells in rats by transforming growth factor beta 1 *Gastroenterology* **107** 1319
 - [30] Martino M M and Hubbell J A 2010 The 12th-14th type III repeats of fibronectin function as a highly promiscuous growth factor-binding domain *Faseb J.* **24** 4711
 - [31] Poniatowski L A, Wojdasiewicz P, Gasik R and Szukiewicz D 2015 Transforming growth factor Beta family: insight into the role of growth factors in regulation of fracture healing biology and potential clinical applications *Mediators Inflamm.* **2015** 137823
 - [32] Williams C G, Kim T K, Taboas A, Malik A, Manson P and Elisseeff J 2003 In vitro chondrogenesis of bone marrow-derived mesenchymal stem cells in a photopolymerizing hydrogel *Tissue Eng.* **9** 679
 - [33] Barry F, Boynton R E, Liu B and Murphy J M 2001 Chondrogenic differentiation of mesenchymal stem cells from bone marrow: differentiation-dependent gene expression of matrix components *Exp. Cell Res.* **268** 189
 - [34] Witte K, Rodrigo-Navarro A and Salmeron-Sanchez M 2019 Bacteria-laden microgels as autonomous three-dimensional environments for stem cell engineering *Mater. Today Bio.* **2** 100011
 - [35] Kanczler J, Tare R S, Stumpf P, Noble T J, Black C and Oreffo R O C 2019 Isolation, differentiation, and characterization of human bone marrow stem cells In vitro and in vivo *Methods Mol. Biol.* **1914** 53
 - [36] Andersen T, Auk-Emblem P and Dornish M 2015 3D cell culture in alginate hydrogels *Microarrays* **4** 133
 - [37] Sart S, Bejoy J and Li Y 2017 Characterization of 3D pluripotent stem cell aggregates and the impact of their properties on bioprocessing *Process Biochem.* **59** 276
 - [38] Cascone S and Lamberti G 2020 Hydrogel-based commercial products for biomedical applications: A review *Int. J. Pharm.* **573** 118803
 - [39] Shao C, Chi J, Zhang H, Fan Q, Zhao Y and Ye F 2020 Development of cell spheroids by advanced technologies *Advanced Materials Technologies* **5** 2000183
 - [40] Jackson-Holmes E L, McDevitt T C and Lu H 2017 A microfluidic trap array for longitudinal monitoring and multi-modal phenotypic analysis of individual stem cell aggregates† *Lab Chip* **17** 3634
 - [41] Paik I, Scurr D J, Morris B, Hall G, Denning C, Alexander M R, Shakesheff K M and Dixon J E 2012 Rapid micropatterning of cell lines and human pluripotent stem cells on elastomeric membranes *Biotechnol. Bioeng.* **109** 2630
 - [42] Yoshimitsu R *et al* 2014 Microfluidic perfusion culture of human induced pluripotent stem cells under fully defined culture conditions *Biotechnol. Bioeng.* **111** 937
 - [43] Gaut C and Sugaya K 2015 Critical review on the physical and mechanical factors involved in tissue engineering of cartilage *Regen. Med.* **10** 665
 - [44] Bornes T D, Jomha N M, Mulet-Sierra A and Adesida A B 2015 Hypoxic culture of bone marrow-derived mesenchymal stromal stem cells differentially enhances in vitro chondrogenesis within cell-seeded collagen and hyaluronic acid porous scaffolds *Stem Cell Res. Ther.* **6** 84
 - [45] Sarem M, Heizmann M, Barbero A, Martin I and Shastri V P 2018 Hyperstimulation of CaSR in human MSCs by biomimetic apatite inhibits endochondral ossification via temporal down-regulation of PTH1R *Proc. Natl Acad. Sci. USA* **115** E6135
 - [46] Centeno C J, Busse D, Kisiday J, Keohan C, Freeman M and Karli D 2008 Regeneration of meniscus cartilage in a knee treated with percutaneously implanted autologous mesenchymal stem cells *Med. Hypotheses* **71** 900
 - [47] Dexheimer V, Frank S and Richter W 2012 Proliferation as a requirement for in vitro chondrogenesis of human mesenchymal stem cells *Stem Cells Dev.* **21** 2160
 - [48] Ballock R T and O'Keefe R J 2003 Physiology and pathophysiology of the growth plate *Birth Defects Res. C* **69** 123
 - [49] Mueller M B, Fischer M, Zellner J, Berner A, Dienstknecht T, Prantl L, Kujat R, Nerlich M, Tuan R S and Angele P 2010 Hypertrophy in mesenchymal stem cell chondrogenesis: effect of TGF-beta isoforms and chondrogenic conditioning *Cells Tissues Organs* **192** 158
 - [50] Salmeron-Sanchez M and Dalby M J 2016 Synergistic growth factor microenvironments *Chem. Commun.* **52** 13327
 - [51] Martino M M *et al* 2011 Engineering the growth factor microenvironment with fibronectin domains to promote wound and bone tissue healing *Sci Transl Med* Vol. **3** 100ra89
 - [52] Studer D, Millan C, Ozturk E, Maniura-Weber K and Zenobi-Wong M 2012 Molecular and biophysical mechanisms regulating hypertrophic differentiation in chondrocytes and mesenchymal stem cells *Eur. Cell Mater.* **24** 118
 - [53] Poole A R, Kojima T, Yasuda T, Mwale F, Kobayashi M and Lavery S 2001 Composition and structure of articular cartilage: a template for tissue repair *Clin Orthop Relat Res* pp S26
 - [54] Wang C C, Yang K C, Lin K H, Liu Y L, Liu H C and Lin F H 2012 Cartilage regeneration in SCID mice using a highly

- organized three-dimensional alginate scaffold *Biomaterials* **33** 120
- [55] Karunanithi P, Murali M R, Samuel S, Raghavendran H R B, Abbas A A and Kamarul T 2016 Three dimensional alginate-fucoidan composite hydrogel augments the chondrogenic differentiation of mesenchymal stromal cells *Carbohydr. Polym.* **147** 294
- [56] van der Kraan P M and van den Berg W B 2012 Chondrocyte hypertrophy and osteoarthritis: role in initiation and progression of cartilage degeneration? *Osteoarthr. Cartil.* **20** 223
- [57] Shen G 2005 The role of type X collagen in facilitating and regulating endochondral ossification of articular cartilage *Orthod. Craniofac. Res.* **8** 11
- [58] Schwartz G K and Shah M A 2005 Targeting the cell cycle: a new approach to cancer therapy *J. Clin. Oncol.* **23** 9408
- [59] Govinden R and Bhoola K D 2003 Genealogy, expression, and cellular function of transforming growth factor-beta *Pharmacol. Ther.* **98** 257
- [60] Sporn M B, Roberts A B, Wakefield L M and Assoian R K 1986 Transforming growth factor-beta: biological function and chemical structure *Science* **233** 532
- [61] Patil V S, Zhou R and Rana T M 2014 Gene regulation by non-coding RNAs *Crit. Rev. Biochem. Mol. Biol.* **49** 16
- [62] Liu X, Fortin K and Mourelatos Z 2008 MicroRNAs: Biogenesis and molecular functions *Brain Pathol.* **18** 113
- [63] Budd E, Waddell S, de Andres M C and Oreffo R O C 2017 The potential of microRNAs for stem cell-based therapy for degenerative skeletal diseases *Curr. Mol. Biol. Rep.* **3** 263
- [64] Karlsen T A, Jakobsen R B, Mikkelsen T S and Brinchmann J E 2014 MicroRNA-140 targets RALA and regulates chondrogenic differentiation of human mesenchymal stem cells by translational enhancement of SOX9 and ACAN *Stem Cells Dev.* **23** 290
- [65] Tuddenham L, Wheeler G, Ntounia-Fousara S, Waters J, Hajihosseini M K, Clark I and Dalmay T 2006 The cartilage specific microRNA-140 targets histone deacetylase 4 in mouse cells *FEBS Lett.* **580** 4214
- [66] Miyaki S *et al* 2009 MicroRNA-140 is expressed in differentiated human articular chondrocytes and modulates interleukin-1 responses *Arthritis Rheum.* **60** 2723
- [67] Budd E, de Andres M C, Sanchez-Elsner T and Oreffo R O C 2017 MiR-146b is down-regulated during the chondrogenic differentiation of human bone marrow derived skeletal stem cells and up-regulated in osteoarthritis *Sci Rep.* **7** 46704
- [68] Eskildsen T, Taipaleenmaki H, Stenvang J, Abdallah B M, Ditzel N, Nossent A Y, Bak M, Kauppinen S and Kassem M 2011 MicroRNA-138 regulates osteogenic differentiation of human stromal (mesenchymal) stem cells in vivo *Proc. Natl Acad. Sci. USA* **108** 6139
- [69] Moshaverinia A, Xu X, Chen C, Akiyama K, Snead M L and Shi S 2013 Dental mesenchymal stem cells encapsulated in an alginate hydrogel co-delivery microencapsulation system for cartilage regeneration *Acta Biomater.* **9** 9343